1 Decay Region and Downstream Detectors

1.1 Vessel, Vacuum System and Magnet

1.1.1 The Vacuum Vessel

The beam & decay vacuum vessel for the NA62 experiment, see Figure 1, is mostly made up of vacuum vessel parts from the NA48 experiment. In the NA48 configuration, the vacuum vessel parts referred to as the 'blue tube' were numbered from 1 to 22. Typically, 6m long cylinders were connected together into couples of 12m length. In the configuration for the NA62 experiment, the cylindrical parts start with number 7 which is positioned 105.595m from the target, and end with the connection window to the new LAV11 at 219.65m, a total length of some 114m.

Figure 1: The NA62 beam & decay vacuum vessel

The vacuum vessel starts in the experimental cavern TCC8 and continues into the cavern ECN3 where the floor is 1.66m lower. The beam axis in TCC8 is 1.2m from the floor whilst in ECN3 it is 2.86m. The bottom of the vacuum vessel in TCC8 is very close to the floor so that the supports of the vessel connect directly to the floor. In the ECN3 cavern, radiation shielding blocks will be used as a means of intermediate support from the floor to the supports of the vacuum vessel, as they were for NA48.

For the purpose of this description, the vacuum vessel can be described in three parts; the sections that are situated in TCN8 with a diameter of 1.92m, the sections situated in ECN3 with a diameter of 2.4m and the sections in ECN3 with a larger diameter 2.8m (the old NA48 helium vessel).

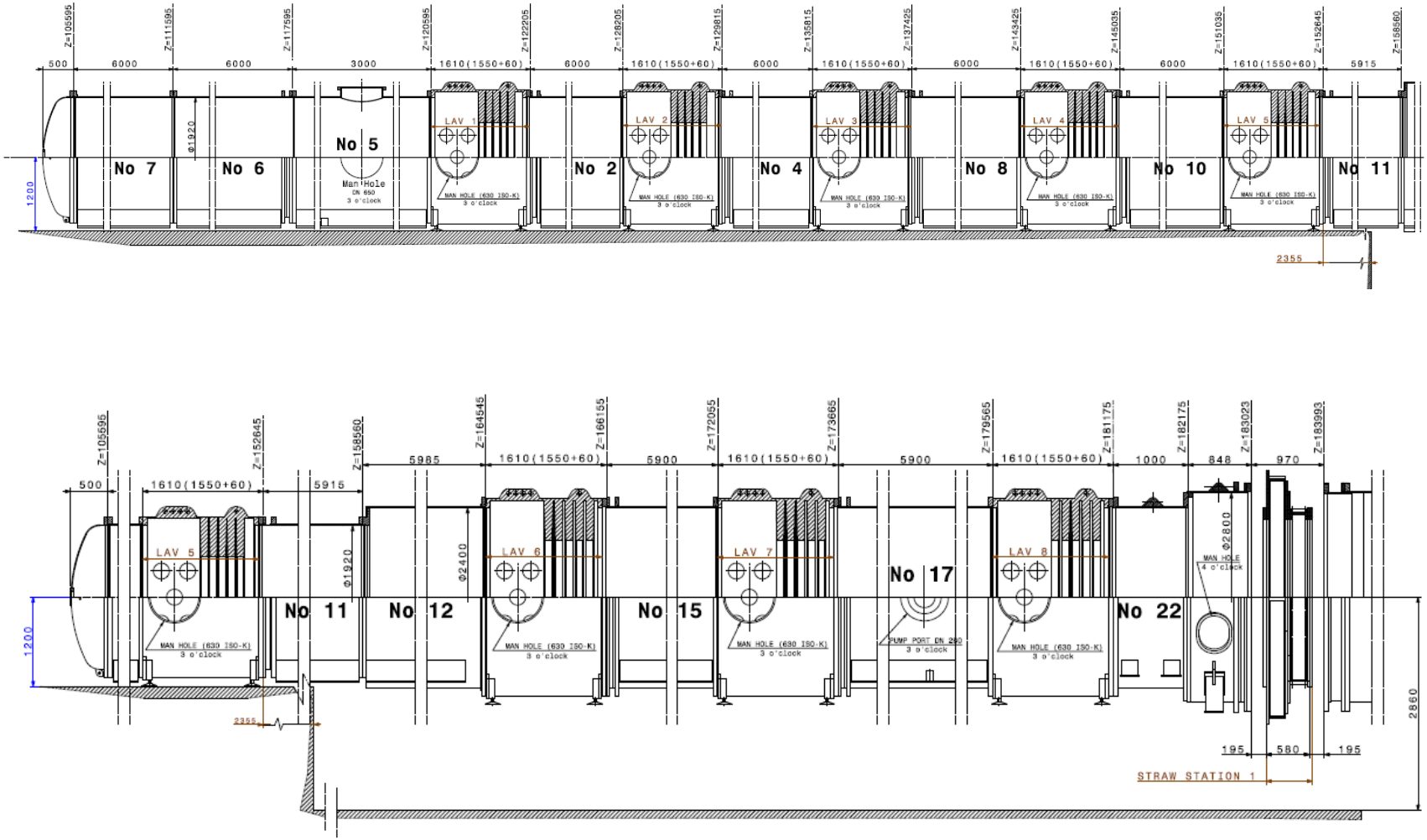

Figure 2 Vacuum vessel sections in TCC8 (parts 7 to 11) and in ECN3 (parts 11 to 22).

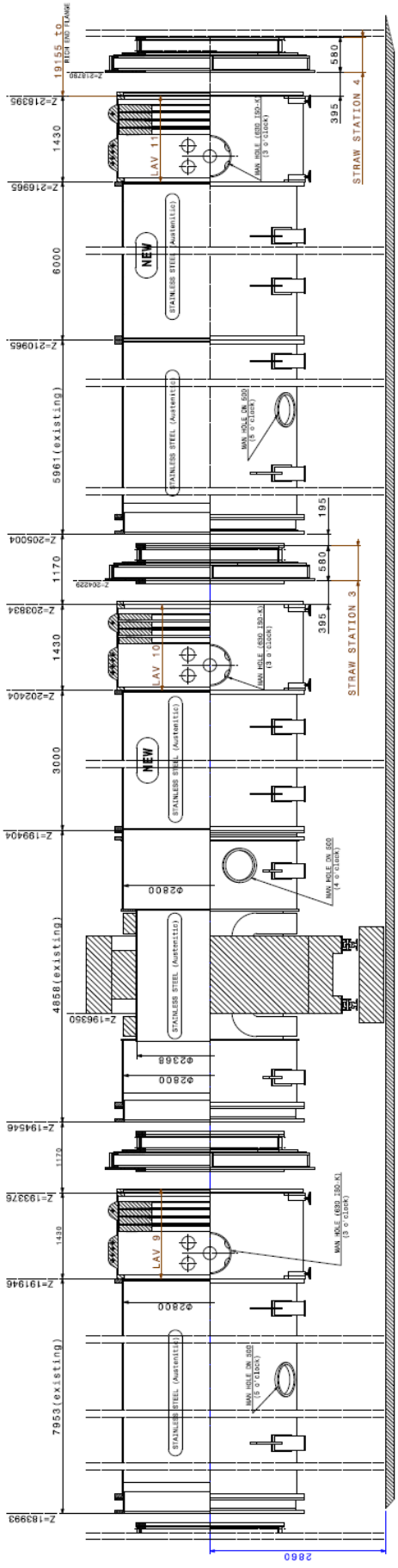

Figure 3 : Vacuum vessel sections in ECN3 of 2.8m diameter that include the MNP33 magnet together with the straw chambers and LAV stations.

The vacuum vessel in TCN8 is made up of the following parts:

- Part 7, 6m length, 1.92m inner diameter
- Part 6, 6m length, 1.92m diameter
- Part 5, 3m length, 1.92m diameter
- Large Angle photon Veto 1 (LAV1), 1.92m diameter (at the connection flange)
- Part 2, 6m length, 1.92m diameter
- LAV 2, 1.92m diameter
- Part 4, 6m length, 1.92m diameter
- LAV 3, 1.92m diameter
- Part 8, 6m length, 1.92m diameter
- LAV 4, 1.92m diameter
- Part 10, 6m length, 1.92m diameter
- LAV 5, 1.92m diameter
- Part 11, 5.915m length, 1.92m diameter (straddles TCN8 and ECN3)

From the above list, and the accompanying Figure 143, it can be seen that: the common diameter is 1.92m, the LAV stations 1-5 are all identical and are spaced apart by 6m long sections of existing 'blue tube'.

The vacuum vessel in ECN3 is made up of the following parts:

- Part 12, 5.985m length, transition piece with diameter increase from 1.92m to 2.4m
- LAV 6, 2.4m diameter
- Part 15, 5.9m length, 2.4m diameter
- LAV 7, 2.4m diameter
- Part 17, 5.9m length, 2.4m diameter
- LAV 8, 2.4m diameter
- Part 22, 1m length, transition piece with diameter increase from 2.4m to 2.8m

From the above list, and the accompanying Figure 144, it can be seen that: the common diameter is 2.4m, the LAV stations 6-8 are all identical and are spaced apart by 5.9m long sections of existing 'blue tube'.

The vacuum vessel containing the magnet spectrometer, the new straw chambers and the LAV's 9, 10 & 11 is made up of the following parts:

- Transition piece (diameter change) 0.848m length, 2.8m diameter
- Straw Chamber 1, 0.970m length (including interface parts)
- 7.953m length, 2.8m diameter, stainless steel
- LAV 9, 2.8m diameter
- Straw Chamber 2, 1.170m length (including interface parts)
- 4.858m length, 2.8m to 2.4m diameter reduction for the MNP33 magnet, stainless steel
- 3m length, new section, 2.8m diameter, stainless steel
- LAV 10, 2.8m diameter
- Straw Chamber 3, 1.170m length (including interface parts)

- 5.961m length, 2.8m diameter
- 6m length, new section, 2.8m diameter, normal steel.
- LAV station 11
- Straw Chamber 4, with connections to LAV 11 and RICH.

From the above list, and the accompanying drawing Figure 144, it can be seen that: the common diameter is 2.8m, the LAV stations 9-11 are all identical, the existing MNP33 magnet is re-used for NA62 and the four straw stations are all in this region. There are also two new vacuum vessel sections of 2.8m diameter required, one 3m long in stainless steel and one 6m long in normal steel.

At the end of this vacuum vessel, and after straw chamber 4, the beam vacuum continues through the RICH detector and the Liquid Krypton calorimeter by means of a beam pipe.

1.1.2 Connections and Adjustment Possibilities

For the NA62 configuration it is common to use 6m long sections of vacuum vessel connecting between LAV stations. Practically every second component (LAV detector or vacuum vessel) has an extendable flange (telescopic extension of the tube) with a sliding vacuum seal. These flanges provide a longitudinal opening of approx. 60mm allowing for lateral extraction e.g. a LAV module. These connections include 'O' ring seals to ensure the leak tightness and fixation bolts to connect the parts together.

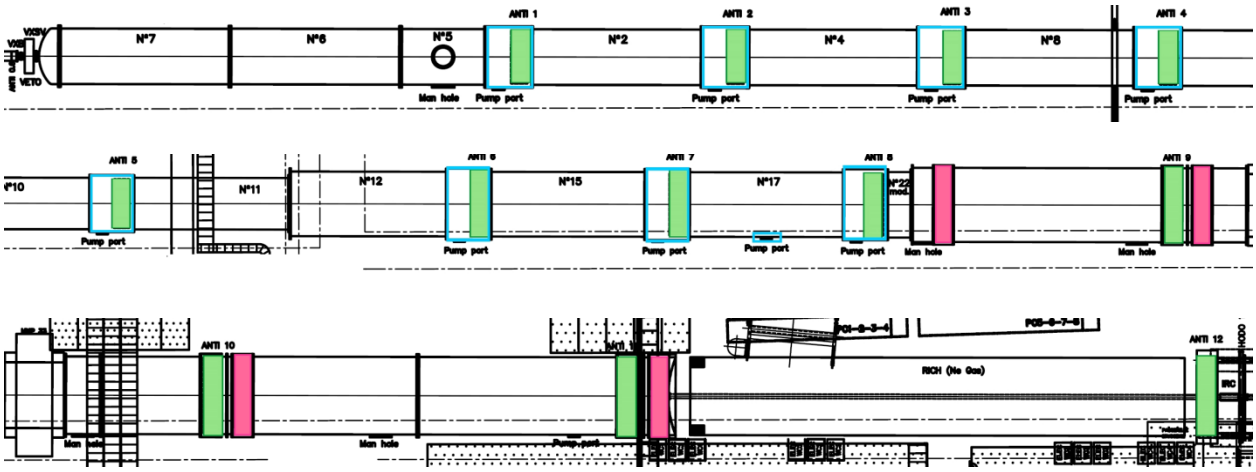

Figure 4: Layout of the decay tube vacuum tank with LAV stations and Straw detectors (in green and pink respectively) Vacuum Requirements

1.2 The Vacuum Pumping System

The beam particles that exit from the beam line at the level of the final collimator are transported towards the main detectors through vacuum. The physics events of interest are kaon decays in the first ~65 metres following the final collimator. Beam particle interactions with the rest gas could cause background events faking the signal of interest. The pressure in the tank must therefore be minimized accordingly. The decay products diverge from the beam axis, the diameter of the decay volume must therefore be sufficiently large to contain the decay products within the detector

acceptance, as well as a number of veto detectors (LAV or Large Angle photon Veto stations). The same beam & decay vacuum tank also houses the four Straw detectors.

1.2.1 Layout

Figure 4 shows the layout of the 480m^3 decay tube volume, where the main new sources of out-gassing are integrated: 12 LAV stations (green) and 4 Straw detectors (pink). The expected gas load is discussed in paragraph 1.2.3. The vacuum tank is made of steel (or stainless steel for the elements around the magnet), painted on the inside, and has a total volume of ~500 m^3.

1.2.2 Vacuum Requirements

A FLUKA simulation has allowed quantifying the effect of interactions of pions, kaons and protons with the residual gas in the decay vacuum tank. The generated beam particle interaction data were passed to a detector simulation where the probability that such an interaction can cause fake triggers, and consequent mis-tagging, was computed. The conclusion of this study is that vacuum in the upstream part of the vacuum tank (that is up to the 1st Straw chamber or a tube length of about 80 m) should be better than 6.10^{-8} mbar to keep the background to less than one fake event per year. With a CEDAR counter positively tagging the 6% of kaons in the beam the accidental mis - tagging is minimized as pion and proton interactions with the rest gas are then mostly rejected. Then the vacuum requirement for the first 80 metres can be reduced to a vacuum of 10^{-6} mbar or better.

The vacuum in the downstream parts of the vacuum tank (spectrometer area) must still be 10^{-5} mbar or better to limit Coulomb scattering between beam particles and the particles present in the blue tube.

In order to design a vacuum system capable of achieving the required vacuum levels we must first evaluate the gas load to the system and then take into account available conductance's for the vacuum tube and the pumping ports.

1.2.3 Gas Load (Out-Gassing and Permeation)

Estimates exist for the three main gas loads based on different sets of measurements that were performed between 2006 and 2010. The two main sources of out-gassing and their estimated out-gassing rates are as follows:

- The vacuum vessel [1] itself (blue tube, painted steel): 10^{-2} mbar l/s
- Set of 12 LAV stations (1): 2-5 10^{-2} mbar l/s

The Straw detectors contribute to the overall gas load of the vacuum tank through permeation of the detector gas through the surface of the Straws. The Straws will either be filled with a CO_2 90%, iC_4H_{10} 5%, CF_4 5% (slow gas) or Ar 70%, CO_2 30% (fast gas) mixture. The proposed vacuum system must be able to meet the vacuum requirements for both Straw mixtures, keeping in mind that the permeation for Argon through the straws is about 1/16 of that for CO_2. As CO_2 has the highest permeation rate of the gases mentioned above, the "slow gas" mixture yields the highest release of

[1] Result from measurements performed in 2006.

CO_2 into the vacuum tank. The Straw detector gas load from permeation (for the "slow gas" mixture) is measured to be 10^{-1} mbar l/s.

Table 1 shows the gas load contributions of the four elements discussed. The last two columns show the fractions of gases which are condensable (non-condensable) at 77K.

Table 1: The gas load, condensable and non-condensable.

	Total gas load [mbar·l·s^{-1}]	Condensable gas load [mbar·l·s^{-1}]	Non condensable gas load [mbar·l·s^{-1}]
Blue tube	10^{-2}	$8 \cdot 10^{-3}$	$2 \cdot 10^{-3}$
LAV	$3 \cdot 10^{-2}$	$2.4 \cdot 10^{-2}$	$6 \cdot 10^{-3}$
Straw (90% CO_2)	$1 \cdot 10^{-1}$	$1 \cdot 10^{-1}$	$3 \cdot 10^{-3}$
Straw (30% CO_2)	$3.4 \cdot 10^{-2}$	$3 \cdot 10^{-2}$	$4 \cdot 10^{-3}$

The gas loads listed above show that Straw trackers dominate the gas load and therefore define the pumping speed needed to match the vacuum requirements. The required pumping speed is then of the order of 150000 l/s.

1.2.4 Conductances

The large cross section of the blue tube, 2.9m^2, or more, gives it nearly zero hydraulic impedance. LAV detectors represent a restriction to a surface of 0.9m^2 or larger. It is assumed that each Straw detector presents an impedance equivalent to 0.2m^2 of free surface. LAVs and Straws can therefore help in establishing a structured pressure profile along the blue tube and in particular, to maintain a pressure difference between the decay region and the Straw region. This throttling may be exploited to restrict the achievement of the more stringent vacuum requirement of 10^{-6}mbar to the decay region instead than to the whole blue tube.

There are twelve manholes of 630mm diameter along the blue tube, corresponding to each LAV detector. Three further pumping ports of 280mm diameter are located at the downstream extremity, in the Straw region. Under the condition that the manholes are easily made available for access and maintenance, all these apertures can be used to install pumping groups.

1.2.5 Technical Pumping Solutions

Two approaches to reach the required vacuum levels are considered, both based on a mixed scheme, with dry pumps and roots pumps for the first level of pumping and then diffusion pumps and/or cryo-pumping for the second level; one solution implements industrial cryo-pumps, while the other foresees diffusion pumps with a custom made cold-trap at liquid nitrogen temperature. It is worth noting that, because of electromagnetic interference with the different tracker detectors in the region, turbo-molecular pumps cannot be used near the blue tube while the detectors are operating.

The main technical principles behind these two cryo-pumping solutions are described here and in the next paragraphs. In both cases, a set of primary dry pumps are used to reach a rough vacuum of ~10^{-3} mbar in the 480m^3 volume. Additional oil diffusion pumps provide part of the required pumping speed. The remainder is ensured by cryo-pumping. In one case, one would use off-the-shelf industrial cryo-pumps in the other cryo-panels, cooled with liquid nitrogen.

1.2.5.1 Industrial Solution

In the first case, a consistent proportion of the pumping speed is provided by off-the-shelf two-stage cryo-pumps, based on the Gifford-MacMahon closed cycle for refrigeration. Helium gas is compressed at warm and expands against a moving piston at cold, providing refrigeration power to a cold-head.

Operating at a temperature below 20K, cryo-pumps feature the highest pumping speed of all industrial vacuum pumps for a given size of pumping port; besides cryo-condensation, acting typically on H_2O, N_2, CO_2 and Ar, cryo-sorption on cold active charcoal provides pumping speed for H_2 and Ne.

Fully automatic operation, including regular regeneration, is ensured by a control unit. A yearly maintenance of the cold-head by specialized personnel is required.

Equipping each cryo-pump with a remotely controlled gate valve allows for the isolation of the pumps from the main vacuum volume for their regeneration during beam time. However, the inclusion of the gate valves will result in a loss of ~30% of pumping efficiency.

1.2.5.2 Custom-Made Solution

At 77K, the liquid nitrogen temperature at normal pressure, CO_2 exhibits a saturation vapour pressure of $2 \cdot 10^{-8}$mbar. With the required vacuum level, it is interesting and cost-effective to apply cryo-pumping only to CO_2 using a large cryo-panel supplied with liquid nitrogen via a small pumping port. Pumping speed is proportional to the cold surface area and can, in principle, be increased at will, limited only by the liquid nitrogen flow needed to maintain a larger panel at the required temperature. In practice, the size of the cold surface is limited by the requirement not to decrease the temperature of the neighbouring LAV detector by more than 20K.

Total capacity is determined by the temperature of the upmost layer of condensed gas, and is therefore limited by the thermal conductance in the condensed layer and the heat load to it. Liquid nitrogen flow, from a Dewar installed in the cavern, would ensure stable temperature conditions by pressure drop, limiting control devices to a flow-regulated warm valve and some temperature sensors.

Laboratory tests on a prototype, scaled down to the NA62 operating conditions, have validated the principle of a liquid nitrogen cooled cryo-panel for CO_2 pumping, confirming that pumping speed, heat losses, capacity and the stability of the system, are sufficient to cope with the required vacuum levels and operation scheme of NA62 (2).

The final choice will strongly depend on the design retained for the Straws and will result from a trade-off between reliability and cost, the latter including equipment, maintenance and operation. A detailed analysis of these aspects is under way. Some preliminary technical considerations must be taken into account to complete this forthcoming analysis.

The throttling effect by the Straws, separating a 10^{-6}mbar region from a 10^{-5}mbar one, is essential in limiting the total required pumping speed and should be validated by numerical calculation or test.

An apparent advantage for the cryo-panel solution, the availability of liquid nitrogen from the neighbouring LKr calorimeter appears, *a posteriori*, impossible to exploit, considering the age and

fragility of the liquid nitrogen feeding system. The purchase and installation of a separate liquid nitrogen storage and transfer system has therefore to be included in the cost estimation. An extended cryo-panel, cooled by a closed-cycle refrigerated cold-head, may represent a valuable alternative to liquid-nitrogen flow. Pumping speed can in principle be increased at will, but it is restricted to a 77K condensable gas species.

In spite of the simplicity of operation, often presented by industry, of off-the-shelf cryo-pumps based on closed-cycle refrigeration, they require regular, costly, maintenance and present an intrinsic fragility, requiring a consistent proportion of installed pumping contingency. The counterpart is a huge, wide-spectrum pumping speed, including air components, where a liquid-nitrogen cooled cryo-panel would ensure a comparably high pumping speed only for CO_2, water and hydrocarbons. In case of an air-leak to the vacuum system, to counterbalance the safety margin ensured by cryo-pumps, an equivalent over-dimensioning of the diffusion-pump system would be necessary in the cryo-panel version. Following this line of reasoning, the cryo-panel solution is particularly adapted to the case of a 90% CO2-filling of permeable Straws, but this may not be optimized to cope with a different filling scheme or a higher permeation by Ar.

There is also the question of contamination, or even saturation, of the cryo-pumping cold surfaces by oil from the diffusion pumps. It is, however, not excluded that special oils with sufficiently low condensation pressures would only have a minimum effect on the cryo-pumping efficiency.

1.3 The MNP33 Magnet

The NA62 experiment uses the same magnet as previously the NA48 experiment, the MNP33. The various parts that make up the magnet have been removed from the beam line and were put to one side. These parts have now been re-assembled in their nominal NA62 position. Some parts of the magnet system – flexible cooling lines for example – will need to be replaced.

This magnet had new coils added at the time of the NA48 experiment. The magnet cross-sectional dimension is 4.4m wide by 4m high and it is 1.3m long. The overall weight of the magnet is 105 tonnes. The main field component goes from top to bottom. Most of the details of the magnet in this section have been extracted from (3).

The iron yoke is made of forged steel. Additional return yokes were added for NA48 with dimensions 3.2m x 0.6m x 1.3m to provide a gap height of 2.40m. The aperture is 3.2m wide.

The helium tank magnet section of NA48 is used again, in a new position for NA62, Figure 5, to cross the magnetic gap and leave an active fiducial region of 2.37m diameter, corresponding to the inner diameter of the old helium tank.

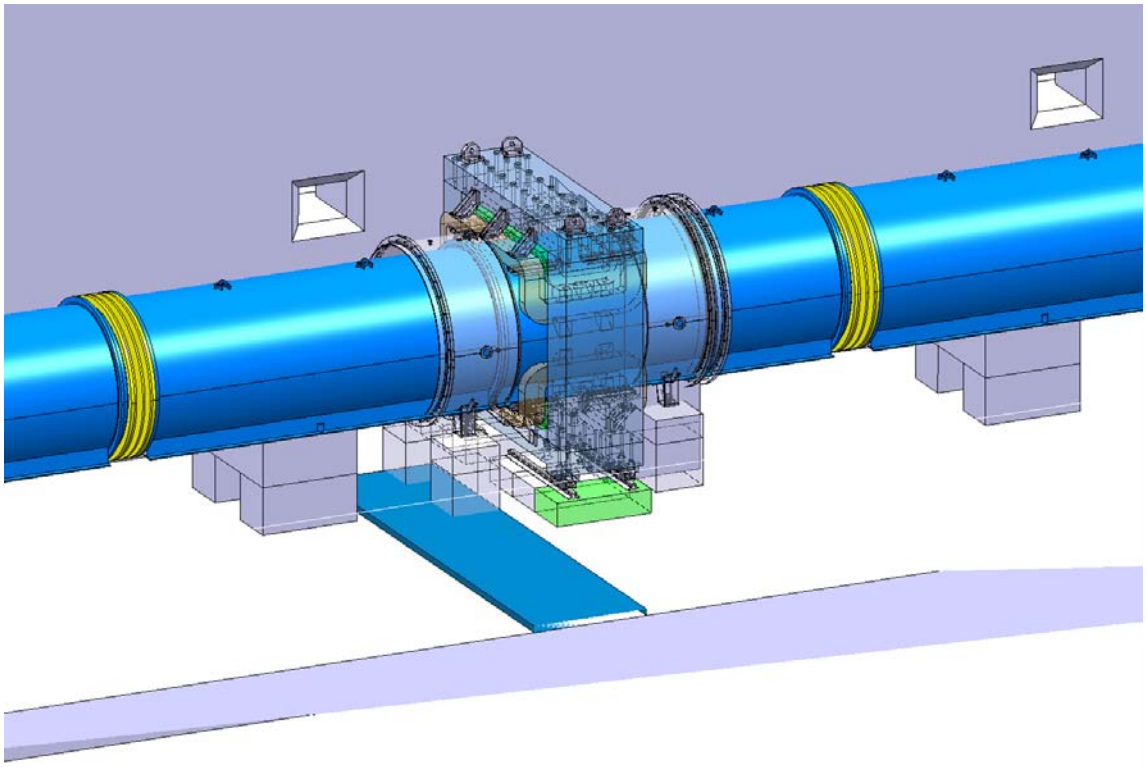

Figure 5: The MNP33 magnet, together with the corresponding section of vacuum vessel (old Helium tank), in its new NA62 position.

1.3.1 The Magnet Coils

The coils are wound with hollow copper conductors of square cross section where cooling water passes through the hollow part. The coils provide an EMF of 0.98 x 10^6 Ampere-turns of which 0.40 x 10^6 are supplied by the original pair and 0.58 x 10^6 by the pair added for NA48. The dissipated power is 3.1 MW. The main parameters of the coils is shown in Table 2.

Table 2: Main parameters of the magnet coils

Coils	Original	Added for NA48	Total
N° of turns	2 x 168	2 x (2 x 120)	816
Nominal current (A)	1200	1200	-
N° of ampere turns (A)	0.4 X 10^6	0.58 X 10^6	0.98 X 10^6
Dissipated power (MW)	1.3	1.8	3.1

Table 3: Main parameters of the conductors

Conductors	Original	Added for NA48
Outer dimensions (mm^2)	14 X 14	15 X 15
Hole diameter (mm)	10	8.5
Net cross-section (mm^2)	117	168
Current density (A/mm^2)	10.2	7.1

1.3.2 The Magnet Power Supply

There are two power supplies that act as master and slave, one for the original and one for the NA48 added coil with a maximum rated current of 1250 and 2500 A respectively. All the coils consist of two parts, upper and lower, electrically connected in series. The newer coil is split into two sections electrically connected in parallel. The main parameters of the conductors is shown in Table 3.

1.3.3 Measured Magnetic Field Parameters

Field calculations and measurements were made in 1995 of the then new magnet configuration. A full field map was measured at the nominal current of 1200A. The measured parameters of the magnet for the nominal operating current are shown in Table 4.

Table 4: Measured parameters of the magnet for the nominal operating current of 1200 A.

Measured field at the centre of the magnet (T)	0.3712
Integrated field (Tm)	0.858
Maximum field close to the poles (T)	<0.9
Maximum field gradient (Tm)	0.9
Transverse momentum (MeV/c)	257.4
Effective magnetic length (m)	2.31

1.3.4 Dismounting and Re-assembly of the Magnet

The magnet has now been disassembled from its previous position in NA48. The following drawing, Figure 6, was made to assist with the disassembly

The magnet has now been reassembled in its new position for NA62. A drawing, Figure 7, was made to show the new position.

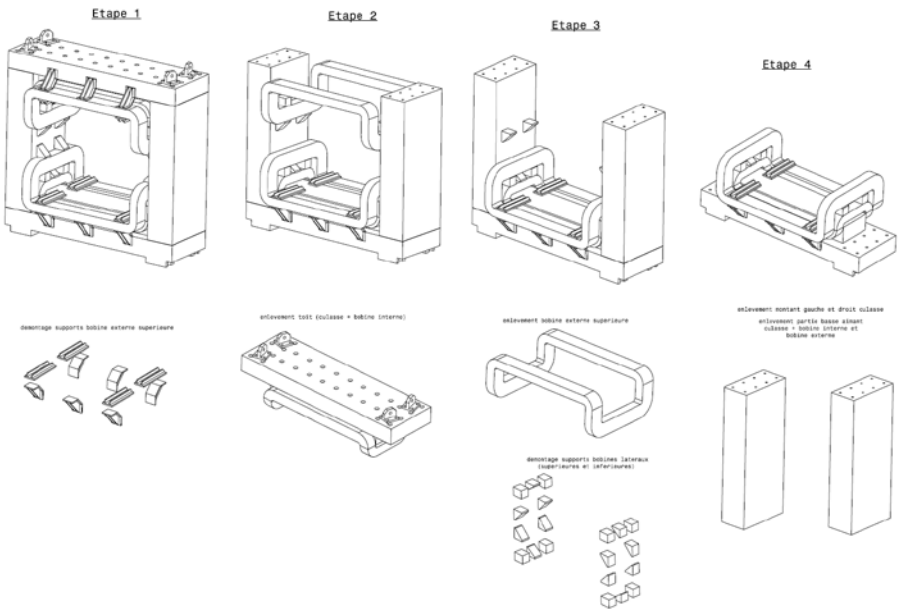

Figure 6: The magnet broken down into its parts

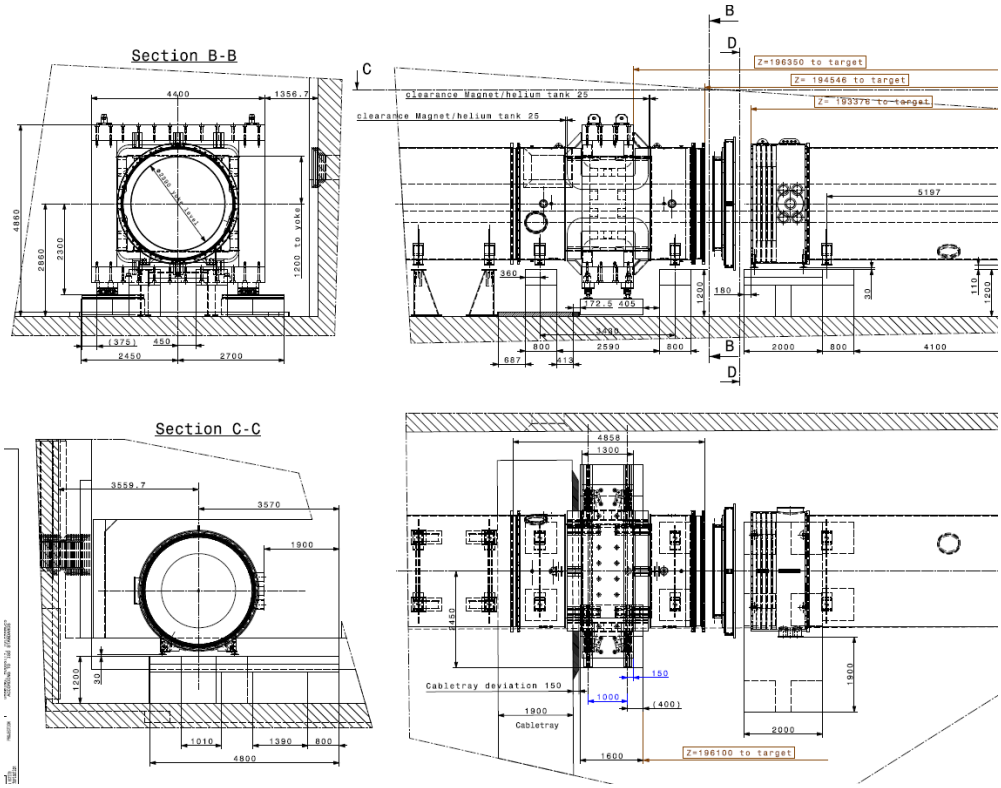

Figure 7: Drawing of the new position of the MNP33 magnet for NA62.

Bibliography

1. **A. Antonelli et al.** Study of the out-gassing rate of the NA62 Large-Angle Photon Veto system. *Internal Note NA62-09-01 .* 2009 йил May.

2. **Jenninger, B. and Vandoni, G.** A Vacuum system for NA62. *CERN Internal Note TE technical note (in preparation).* 2010 йил.

3. *Comparison of field calculations and measurements of a spectrometer magnet.* **Bergsma, F., et al.** Nuclear Instruments and Methods in Physics Research A, s.l. : Elsevier Science B.V., 1995 йил, Vols. A 361 (1995) 466-471. SSDI 0168-9002(95)00142-5.